Biosensors and Bioelectronics 79 (2016) 656–660

Contents lists available at ScienceDirect

Biosensors and Bioelectronics

journal homepage: www.elsevier.com/locate/bios

Designed diblock hairpin probes for the nonenzymatic and label-free detection of nucleic acid

Junlin Wen [a,b,c], Junhua Chen [b,*], Li Zhuang [b], Shungui Zhou [b,*]

[a] Guangzhou Institute of Geochemistry, Chinese Academy of Sciences, China
[b] Guangdong Key Laboratory of Agricultural Environment Pollution Integrated Control, Guangdong Institute of Eco-Environmental and Soil Sciences, Guangzhou 510650, China
[c] University of Chinese Academy of Sciences, Beijing, China

ARTICLE INFO

Article history:
Received 20 November 2015
Received in revised form
28 December 2015
Accepted 29 December 2015
Available online 30 December 2015

Keywords:
Colorimetric assay
Branched DNA junction
Gold nanoparticles
Catalytic hairpin assembly
Shewanella oneidensis

ABSTRACT

The detection of nucleic acid sequences is of great importance in a variety of fields. An ultrasensitive DNA sensing platform is constructed using elaborately designed diblock hairpin probes (DHPs) that are composed of hairpin and poly-adenine blocks. The introduction of an initiator DNA target triggers the catalytic assembly of probes DHP1, DHP2 and DHP3 to fabricate numerous poly-adenine-tailed branched DNA junctions, which significantly amplify the signal of the target-DNA-recognizing event without any enzyme. Coupled to a gold nanoparticle-based colorimetric assay, the amplified recognition signal can be quantitatively detected or visually read with the naked eye. The combination of the high-efficiency target-catalyzed DHP assembly and sensitive gold-based colorimetric assay offers an ultrasensitive detection of DNA with a detection limit of 0.1 pM and a dynamic range from 0.01 to 5 pM. The proposed sensing platform can discriminate even single-base mutations. Moreover, the sensing platform can be expanded to detect pollutant-degrading-bacteria-specific DNA sequences. The proposed sensing system should offer an alternative approach for the detection of nucleic acids in the fields of microbiology, biogeochemistry, and environmental sciences.

1. Introduction

Sequence-specific methods for detecting nucleic acids are critical for medical diagnostics (Jung and Ellington, 2014), food safety (Kim et al., 2014) and environmental science (Tadmor et al., 2011). Many detection systems have been developed by making use of enzymes as amplifiers because of the low abundance of targets in natural environments. Amplificatory tools, such as polymerase (Manrao et al., 2012), ligase (Shen et al., 2012; Wee et al., 2012) and exonuclease (Ju et al., 2012; Xuan et al., 2012), in DNA detection offer exquisite sensitivity and are commonly used to follow target–probe hybridization. However, these enzyme-based assays are labor-intensive, require complex operation, and have a relatively high cost. In contrast, catalytic hairpin assembly (CHA) is a simple and enzyme-free amplifying strategy that can effectively amplify and transduce the signal from DNA hybridizing events (Yin et al., 2008; Jiang et al., 2013b; Chen et al., 2015b). The CHA employs the target-initiated circular assembly of metastable hairpin probes to fabricate branched DNA junctions. Its feasibility to encode DNA functional and structural information, together with catalytic amplification with negligible background, offers unique features for point-of-case analyte detection. In fact, CHA has been used to transduce analyte-recognizing event to a variety of detection modalities, such as electrochemical chemiluminescence (Chen et al., 2015a), electrochemistry (Zhang et al., 2015) and photo-luminescence (Fu et al., 2013). Although these detection techniques are sensitive, their requirements for advanced instrumentations have to some extent limited the field applications.

Gold nanoparticle (AuNP)-based colorimetric detection techniques require simple instrumentation and can be easily read with the naked eye. AuNP colorimetric assays, when coupled with CHA, have seen significant applications in the detection of DNA sequences because target hybridization can be easily transformed to color changes (from red to blue). These assays are commonly realized by modifying a thiolated DNA probe on the surface of AuNPs through the well-established strong Au–S chemistry such that target–probe cross-linking induces their aggregation (Deng et al., 2012; Su et al., 2015). However, cross-link-based methods frequently suffer from being too time consuming (20–40 h) for the preparation of AuNP–DNA conjugates (Xia et al., 2010) due to the tedious process of Au–S chemistry-dependent modification.

* Corresponding authors.
E-mail addresses: jhchen@soil.gd.cn (J. Chen), sgzhou@soil.gd.cn (S. Zhou).

http://dx.doi.org/10.1016/j.bios.2015.12.104
0956-5663/

Moreover, these methods have relatively poor detection limits (low nanomolar). Poly adenine (polyA), a recently reported linker between AuNPs and DNA, has shown a similar affinity to the thiol group (Jiang et al., 2013a; Chen et al., 2014). In addition, polyA requires no modification during synthesis, reducing the cost of detection. Moreover, polyA-mediated binding could be easily modulated (Zhang et al., 2012) and in fact has been used for the preparation of DNA–AuNP conjugates (Pei et al., 2012). However, polyA has not been exploited for the design of a diblock hairpin probe, coupling to CHA reaction, for the development of a nonenzymatic and label-free nucleic acid assay.

In this work, novel diblock hairpin probes composed of hairpin and polyA blocks were elaborately designed. In the presence of target DNA, the designed probes (DHP1, DHP2 and DHP3) are able to construct branched DNA junctions that possess tails of polyA, which can bind on the surface of AuNPs and aggregate them, triggering a color change in the colloidal gold solution. Based on these versatile probes, a nonenzymatic and label-free sensing platform was developed to detect DNA for the first time. Due to the high efficiency of target-triggered catalytic diblock hairpin probe assembly and the sensitive AuNP-based colorimetric assay, a significantly enhanced sensitivity was achieved. Furthermore, the proposed platform exhibited high specificity and was capable of identifying a target from single base mutations. The proposed detection system provides an ultrasensitive sensing platform for the detection of nucleic acid.

2. Materials and methods

2.1. Reagents and materials

The oligonucleotides were synthesized and purified by Sangon Biotech Co. (Shanghai, China), and the sequences are presented in Table S1. Chloroauric acid ($HAuCl_4$) and trisodium citrate were purchased from Sigma-Aldrich (St. Louis, MO). Other common regents were used as received. All of the solutions were prepared using ultra-pure quality water (18.2 MΩ cm resistivity) obtained from a Milli-Q Water System (Millipore Corporation, Bedford, USA).

2.2. Synthesis of gold nanoparticles

AuNPs (15 nm) were prepared by the typical citrate reduction of $HAuCl_4$ according to a previous report (Li and Rothberg, 2004). Briefly, a 5-mL aqueous solution of sodium citrate (1 wt%) was added to a boiling solution of $HAuCl_4$ (100 mL, 0.01 wt%). After the solution color changed to red, the reaction mixture was allowed to boil for 30 min. Then, the synthesized gold solution was cooled to room temperature and stored at 4 °C before use. All of the glassware that was used in the synthesis was cleaned with aqua regia and rinsed with pure water.

2.3. Gel electrophoresis

Lyophilized oligonucleotides were dissolved in ultra-pure water to prepare concentrated DNA stock solutions and later diluted to reaction conditions (50 mM Na_2HPO_4, 1 M NaCl, pH 6.8). The oligonucleotides (probes DHP1, DHP2 and DHP3) were heated to 95 °C for 5 min and then slowly cooled to room temperature and stored at 4 °C prior to use. The target DNA (200 nM) was mixed with 1 μM (final concentration) each of the annealed probes (DHP1, DHP2 and DHP3) and incubated at 25 °C for 2 h. A 3% agarose gel was prepared using TAE buffer (40 mM Tris AcOH and 2.0 mM Na_2EDTA, pH 8.5). The samples were first mixed with loading buffer (V/V, 1:5) and then added to the gel (5 μL per sample). After running at 120 V for 30 min, the gel was photographed in a Gel Doc XR+ system (Bio-Rad).

2.4. Transmission electron microscopy analysis (TEM)

A TEM analysis was performed according to a previous protocol (Deng et al., 2005). The samples that were used for the TEM analysis were prepared by dropping onto copper grids (10 μL per sample). After drying at room temperature, TEM images were taken with a Jeol JEM-2011 (Jeol Ltd., Japan) that was operated at 80 kV in bright-field mode.

2.5. Assay procedure

To begin, 32 μL of each 3-μM annealed hairpin probe and 224 μL of buffer (50 mM Na_2HPO_4 and 1 M NaCl, pH 6.8) were added in a 1.5-mL tube. After mixing with a pipettor, the mixture was aliquoted into eight separate tubes (36 μL per tube). To these tubes, 4 μL each of 50 pM, 30 pM, 10 pM, 5 pM, 3 pM, 1 pM, 0.5 pM and 0.1 pM target DNA was added to reach a total volume of 40 μL. These samples were then mixed and allowed to react for 2 h at room temperature. Subsequently, 30 μL of the prepared reaction mixture was added to an AuNP solution of 270 μL. After incubating for 3 min, the mixed solutions were measured using a TU-1900 UV–vis spectrometer (Beijing, China).

3. Results and discussion

3.1. Principle of the proposed sensing method

The designed DHPs comprise two concatenated domains: a polyA anchoring block and a functional hairpin block (Scheme 1a, left). The hairpin blocks of DHPs contain toeholds (a special nucleation site), denoted a, b and c. The relationships between the segments of DHPs are specified (Scheme 1a, right). In the absence of target DNA (initiator, I), the DHPs are kinetically impeded from forming branched junction, leaving the gold solution remained red (Scheme 1b, left). The assembly of branched DNA junctions occurs when initiator strand I, containing an exposed toehold a*, nucleates at the toehold of DHP1 and initiates a branch migration that opens the hairpin block, forming complex I/DHP1. The complex I/DHP1 has a newly exposed toehold b* that catalyzes the assembly of DHP2 to form I/DHP1/DHP2 and exposes toehold c*, which catalyzes the assembly of DHP3 to form I/DHP1/DHP2/DHP3. Following the above assembly steps, a disassembly step occurs, in which DHP3 replaces I from the complex I/DHP1/DHP2/DHP3, freeing I to initiate the additional assembly of branched junctions (Yin et al., 2008). The produced DNA junctions (DHP1/DHP2/DHP3) possess polyA tails that can combine multiple AuNPs and thereby aggregate them. This polyA-tailed DNA junction induced the aggregation of AuNPs, resulting in the color changing from red to blue (Scheme 1b, right). Because the color change is dynamically dependent on the concentration of target DNA, the proposed sensing system allows for the qualitative and quantitative detection of DNA.

3.2. Evaluation of the proposed sensing platform

The above mentioned mechanism was evaluated using target DNA as an analyte. Fig. 1a shows that color changes from red to blue in the presence of target DNA, whereas the control (without target) remains the characteristic wine red (inserted photo). This result is confirmed in the UV–vis absorption spectra, where the target sample displays absorption at 650 nm attributed to the surface plasmon resonance (SPR) absorption of aggregated AuNPs,

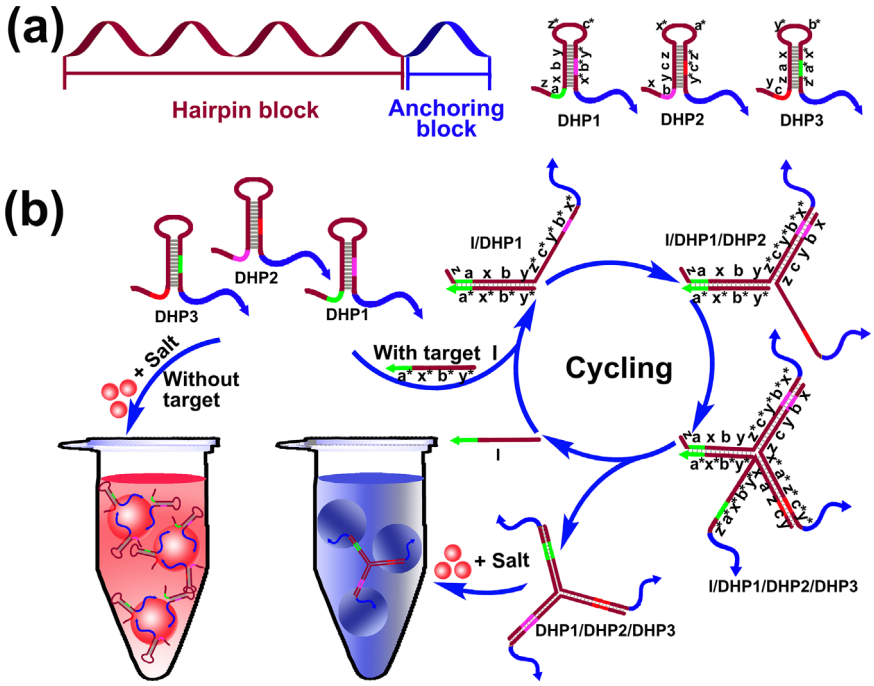

Scheme 1. Schematic illustration of the proposed DNA-sensing platform. (a) Design of diblock hairpin probes consisting of a polyA anchoring block and a hairpin block. (b) Color development of the proposed method in the presence or absence of the target. (For interpretation of the references to color in this figure legend, the reader is referred to the web version of this article.)

while the control presents absorbance at 524 nm, which is the SPR absorption of AuNPs. The corresponding TEM images demonstrate the DNA junction-triggered aggregation of AuNPs. As shown in Fig. 1, AuNPs are monodisperse without target DNA (Fig. 1b) and aggregate as the target present (Fig. 1c). These results are consistent with a previous report (Liu et al., 2013).

To further confirm the assembly of branched DNA junctions, agarose gel electrophoresis was carried out. Target DNA was used as an initiator to trigger the assembly reaction. As shown in Fig. 1d, lane 1 is probe DHP1. When mixed with initiator I, I and DHP1 form the I/DHP1 complex, resulting in lane 2. The successive additions of DHP2 and DHP3 produce complexes of I/DHP1/DHP2 (lane 3) and DHP1/DHP2/DHP3 (lane 4), respectively, which correspond to the intermediate and branched DNA junction. This result demonstrates the successful assembly of DNA junctions.

To demonstrate that polyA tailed hairpin probes are able to prevent AuNPs from salt-induced aggregation, different DNA samples were prepared and mixed with AuNP solutions: sample 1, pure water without salt; sample 2, DHP1 with salt; sample 3, DHP2 with salt; sample 4, DHP3 with salt; and sample 5, DHP1/DHP2/DHP3 (polyA tailed DNA junction) with salt. After incubating at 25 °C for 3 min, sample 1, as shown in Fig. 2, remains the characteristic red color, while samples 2–4 have only a slight color change and sample 5 turns blue. These results demonstrate that the polyA tail of DHP1, DHP2 and DHP3 can stabilize AuNPs (samples 2, 3, and 4), and that the polyA-tailed DNA junction is cable of aggregating gold colloid (sample 5). To precisely assess the aggregation state of gold particles, the ratio of absorbance at 650 *vs* 524 nm ($R_{650/524}$) was used to describe the degree of AuNP aggregation.

3.3. Optimization of assay conditions

Several parameters, including the concentration of the diblock hairpin probes, the reaction time of branched DNA junction assembly, the length of the polyA tail and the concentration of sodium chloride, were optimized using 5 pM target DNA as an analyte. The concentration of diblock hairpin probes is a critical factor that can affect the analytical performance. In the present study, the effect of probe concentration on the responsive colorimetric signal ($R_{650/524}$) was investigated. As shown in Fig. S1, the signal decreases rapidly as the concentration of diblock hairpin probes increases from 100 to 500 nM, while the corresponding control (without target) slowly levels off to a saturation value when the probe is higher than 300 nM. Therefore, 300 nM is selected as the optimal concentration for the following experiments. The reaction time of the DNA junction assembly can also affect the detection sensitivity. As Fig. S2 shows, the detection signal (in the presence of 5 pM target) increases rapidly as the reaction time varies from 60 to 150 min, peaking at 120 min, after which the signal levels off, indicating that the assembly reached its equilibrium. However, the $R_{650/524}$ of the controls without target (background) increases slowly with the increasing reaction time. To obtain the maximal signal amplification and minimal background, 120 min is selected as the reaction time for the following experiments. Although this reaction time seems longer, a significantly amplified responding signal can be obtained. The length of the polyA tail is also important for the assay and was therefore investigated. The results (Fig. S3) show that the $R_{650/524}$ increases gradually as the length of polyA tail increases from 5 to 15 and then levels off. Thereby, hairpins tailed with 15 adenine nucleotides were used in the following study. Furthermore, the NaCl concentration can also impact the detection performance and was consequently evaluated in this study. As Fig. S4 describes, the signal value first increases and then decreases with an increasing NaCl concentration, peaking at 1000 mM. As a result, 1000 mM salt is considered the optimal concentration for AuNP aggregation.

3.4. Specificity evaluation

To investigate the specificity of the proposed method, samples that contained target DNA sequences with matched, mismatched, inserted and deleted base were measured. As shown in Fig. 3, a strong detection signal occurs when the matched target is present,

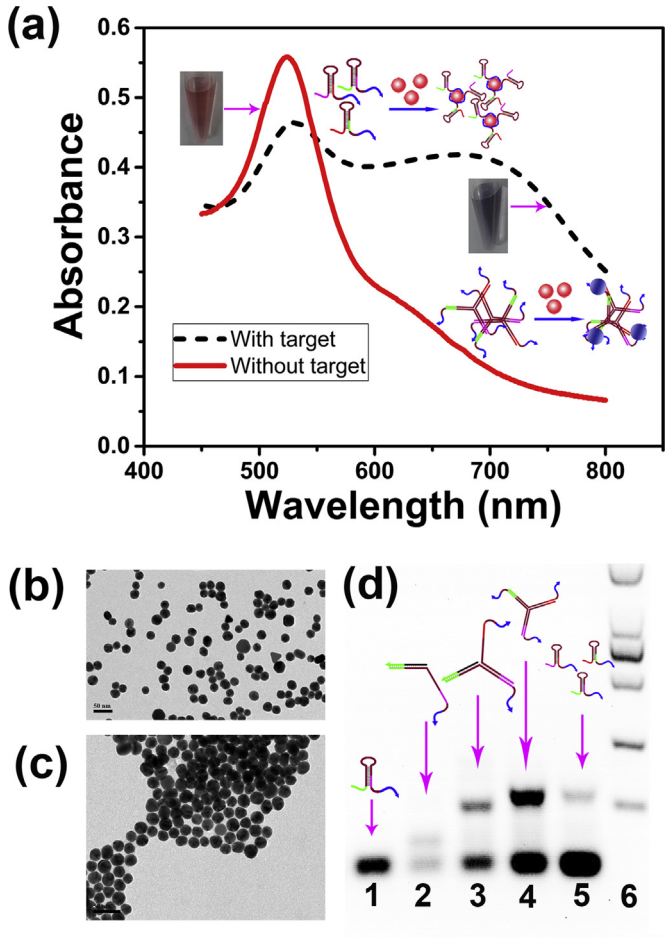

Fig. 1. Evaluation of the proposed platform. (a) UV–vis spectrum of the proposed colorimetric detection system in the absence of target DNA and in the presence of 5 pM target DNA. Inset: photographs. (b) TEM photographs of AuNP solution without target DNA and (c) in the presence of 5 pM target. (d) Gel electrophoresis images for the catalytic diblock hairpin assembly. Lanes: (1) DHP1; (2) DHP1+I; (3) DHP1+DHP2+I; (4) DHP1+DHP2+DHP3+I; (5) DHP1+DHP2+DHP3; and (6) Marker.

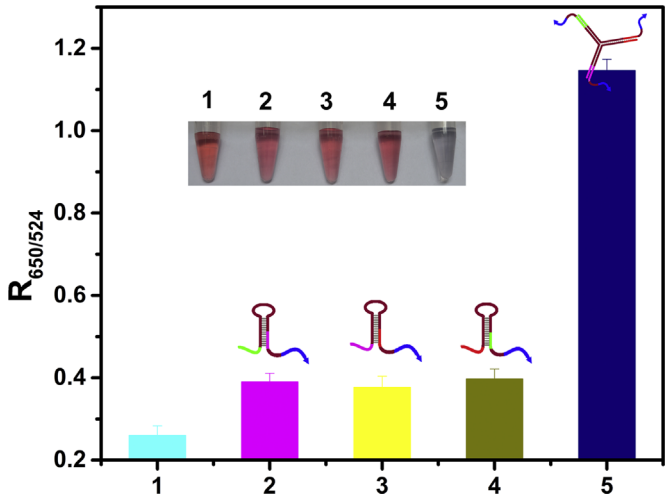

Fig. 2. Colorimetric responses of AuNP solution after adding various oligonucleotides: (1) pure water without salt; (2) DHP1 with salt; (3) DHP2 with salt; (4) DHP3 with salt; and (5) DHP1/DHP2/DHP3 with salt. Error bars were obtained from three independent experiments. Inset: corresponding photograph. (For interpretation of the references to color in this figure, the reader is referred to the web version of this article.)

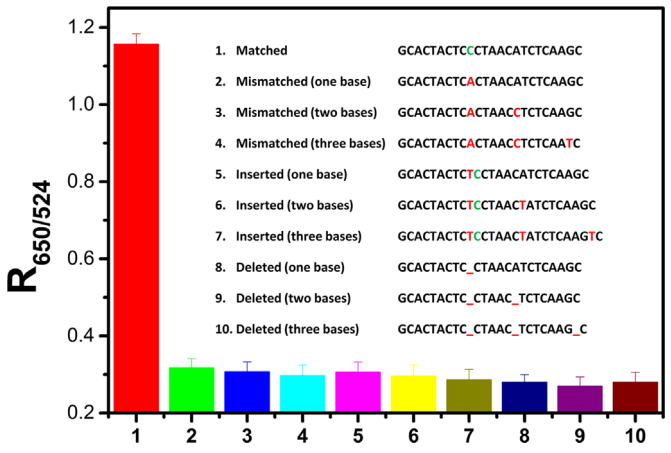

Fig. 3. Colorimetric response of mutated target DNA strands. DNA sequences with matched, mismatched, inserted and deleted bases were used in the measurements.

whereas there are only minor signals in the presence of control DNA sequences (targets with one, two or three bases mismatched, inserted and deleted). This result demonstrates the high specificity of the proposed method.

3.5. Analytical performance

Under optimal conditions, the detection range and sensitivity of the proposed method were determined with varying amounts of target DNA as an analyte. Fig. 4a shows a photograph of AuNPs that were added to the target DNA at concentrations ranging from 0.01 to 5 pM. The color changed from red to blue with the increasing target. The color-developed solutions were measured using UV–vis spectroscopy, and the results are shown in Fig. 4b. Along with the increasing DNA concentration, a novel absorption at 650 nm appeared and increased gradually, while the absorbance at 524 nm gradually decreased. Correspondingly, the ratio of absorbance at 650 nm *vs* 524 nm increased as the amount of target increased. By plotting as in Fig. 4c, a linear relationship can be described using the linear regression equation $Y=0.5927X+0.2753$, where Y is the $R_{650/524}$, and X is the target between 0.01 and 0.5 pM. The detection limit is calculated as 0.1 pM based on three times the standard deviation of the blank measurement, which is beneficial compared to that of a similar method (Table S2). These results indicate that the proposed method is sensitive for detecting DNA.

3.6. Detection of a DNA sequence specific to Shewanella oneidensis

The proposed colorimetric detection method was expanded to detect DNA sequences that were specific to *S. oneidensis*, a versatile pollutant-degrading bacteria (Marshall et al., 2006; Wen et al., 2014; Zhou et al., 2015). The used target DNA sequence is a partial copy of the gene of the extracellular iron oxide respiratory system surface decaheme cytochrome c component (positions 1321–1345 according to the 5′–3′ nucleotide sequence) specific to outer membrane electron transfer: *S. oneidensis* specific target DNA, 5′-TGGTCA-ATGTGT-TCTAGC-GAAGGT-3′. The corresponding diblock hairpin probes were carefully designed: DHP1*, 5′-ATTGGA-ACCTTC-GCTAGA-ACACAT-TGACCA-TCCAAT- CACAAC-TGGTCA-ATGTGT-TCTAGC-A_{15}-3′; DHP2*, 5′-GCTAGA-ACACAT-TGACCA-GTTG TG-ATTGGA-ACACAT-GAAGGT-TCCAAT-CACAAC-TGGTCA-A_{15}-3′; DHP3*, 5′-TGACCA- GTTGTG-ATTGGA-ACCTTC-ATGTGT-TGGTCA-ATGTGT-TCTAGC-GAAGGT-TCCAAT-A_{15}-3′. The introduction of target activates the successive assembly of the probes DHP1*, DHP2* and DHP3*, persistently producing branched DNA

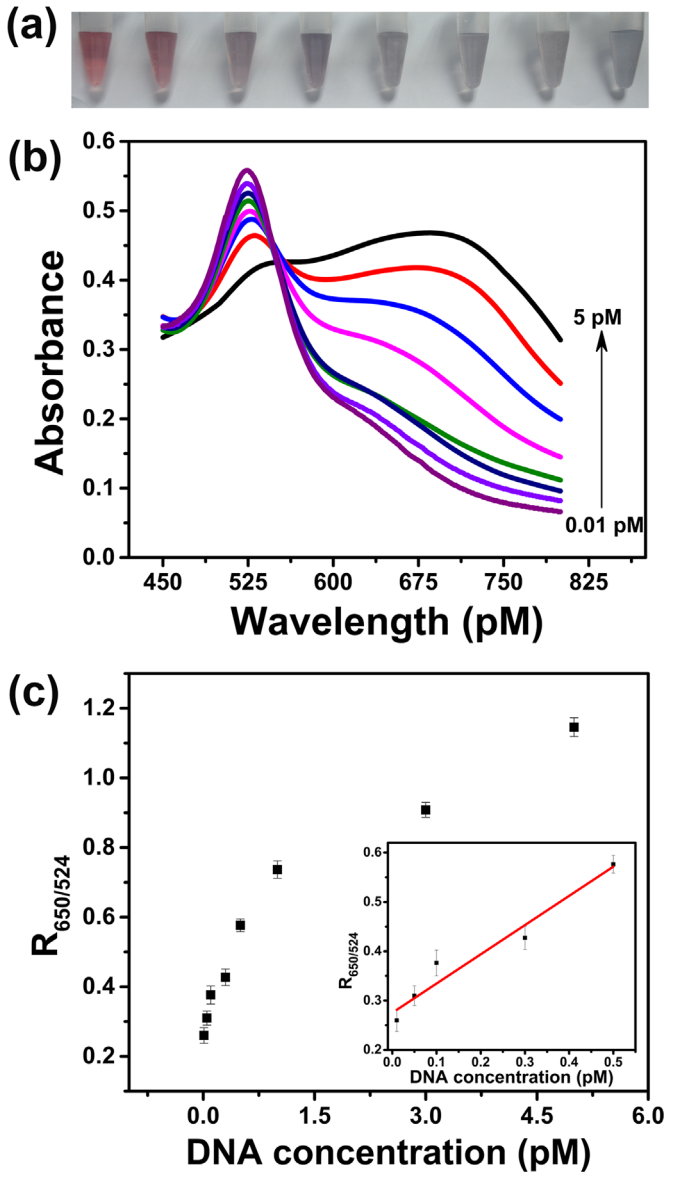

Fig. 4. Colorimetric responses of the proposed detection system in the presence of varied concentrations of the target. (a) Photograph of the AuNP-based detection of DNA. From left to right were 0.01, 0.05, 0.1, 0.3, 0.5, 1.0, 3.0, and 5.0 pM target DNA. (b) UV–vis absorption spectra of the reaction mixture incubated with AuNP solution. (c) Plot of absorbance ratio ($R_{650/524}$) *vs* DNA concentration. The inset is the calibration curve for the target between 0.01 and 0.50 pM.

junctions (Fig. S5a). Using the same scheme, a naked eye assay demonstrated a visible color change of the AuNPs as observed in the absence or presence of target DNA (Fig. S5b). These results indicate that the proposed method is feasible and can be widely used to detect DNA sequences.

4. Conclusion

In conclusion, we have successfully designed novel diblock hairpin probes and constructed a label-free and nonenzymatic DNA-sensing platform by coupling an AuNP colorimetric assay with target-catalyzed hairpin assembly. The combination of the sensitive and convenient gold-based assay and the significant signal amplification of CHA offers several advantages: visual detection, ultrahigh sensitivity, and one base mutation discrimination. Moreover, the established method can be expanded for the detection of *S. oneidensis*-specific DNA sequences. Overall, this colorimetric detection method is simple, inexpensive, and suitable for both qualitative and quantitative assays. The developed sensing platform should offer an alternative approach for the detection of DNA in the fields of microbiology, biogeochemistry, and environmental sciences.

Acknowledgments

This work was supported by the National Natural Science Foundation of China (Grant nos. 41401261 and 21407029), the Science and Technology Program of Guangzhou (Grant no. 201508020010), the Key Projects in the National Science & Technology Pillar Program of China (Grant no. 2015BAD06B03), the Pearl River S&T Nova Program of Guangzhou (Grant no. 201506010093), and the Natural Science Foundation of Guangdong Province (Grant no. 2014A030313705).

Appendix A. Supplementary material

Supplementary data associated with this article can be found in the online version at http://dx.doi.org/10.1016/j.bios.2015.12.104.

References

Chen, J., Qiu, H., Zhang, M., Gu, T., Shao, S., Huang, Y., Zhao, S., 2015a. Biosens. Bioelectron. 68, 550–555.
Chen, J., Zhou, S., Wen, J., 2015b. Angew. Chem. 127 (2), 456–460.
Chen, N., Wei, M., Sun, Y., Li, F., Pei, H., Li, X., Su, S., He, Y., Wang, L., Shi, J., 2014. Small 10 (2), 368–375.
Deng, H., Xu, Y., Liu, Y., Che, Z., Guo, H., Shan, S., Sun, Y., Liu, X., Huang, K., Ma, X., 2012. Anal. Chem. 84 (3), 1253–1258.
Deng, Z., Tian, Y., Lee, S.H., Ribbe, A.E., Mao, C., 2005. Angew. Chem. 117 (23), 3648–3651.
Fu, B., Cao, J., Jiang, W., Wang, L., 2013. Biosens. Bioelectron. 44, 52–56.
Jiang, H., Materon, E.M., Sotomayor, M.D.P.T., Liu, J., 2013a. J. Colloid Interface Sci. 411, 92–97.
Jiang, Y., Li, B.L., Milligan, J.N., Bhadra, S., Ellington, A.D., 2013b. J. Am. Chem. Soc. 135 (20), 7430–7433.
Ju, E., Yang, X., Lin, Y., Pu, F., Ren, J., Qu, X., 2012. Chem. Commun. 48 (95), 11662–11664.
Jung, C., Ellington, A.D., 2014. Acc. Chem. Res. 47 (6), 1825–1835.
Kim, T.-H., Park, J., Kim, C.-J., Cho, Y.-K., 2014. Anal. Chem. 86 (8), 3841–3848.
Li, H., Rothberg, L., 2004. Proc. Natl. Acad. Sci. USA 101 (39), 14036–14039.
Liu, P., Yang, X., Sun, S., Wang, Q., Wang, K., Huang, J., Liu, J., He, L., 2013. Anal. Chem. 85 (16), 7689–7695.
Manrao, E.A., Derrington, I.M., Laszlo, A.H., Langford, K.W., Hopper, M.K., Gillgren, N., Pavlenok, M., Niederweis, M., Gundlach, J.H., 2012. Nat. Biotechnol. 30 (4), 349–353.
Marshall, M.J., Beliaev, A.S., Dohnalkova, A.C., Kennedy, D.W., Shi, L., Wang, Z., Boyanov, M.I., Lai, B., Kemner, K.M., McLean, J.S., 2006. PLOS Biol. 4, e268.
Pei, H., Li, F., Wan, Y., Wei, M., Liu, H., Su, Y., Chen, N., Huang, Q., Fan, C., 2012. J. Am. Chem. Soc. 134 (29), 11876–11879.
Shen, W., Deng, H., Gao, Z., 2012. J. Am. Chem. Soc. 134 (36), 14678–14681.
Su, F., Wang, L., Sun, Y., Liu, C., Duan, X., Li, Z., 2015. Chem. Commun. 51 (16), 3371–3374.
Tadmor, A.D., Ottesen, E.A., Leadbetter, J.R., Phillips, R., 2011. Science 333 (6038), 58–62.
Wee, E.J., Shiddiky, M.J., Brown, M.A., Trau, M., 2012. Chem. Commun. 48 (98), 12014–12016.
Wen, J., Zhou, S., Chen, J., 2014. Sci. Rep. 4, 5191.
Xia, F., Zuo, X., Yang, R., Xiao, Y., Kang, D., Vallée-Bélisle, A., Gong, X., Yuen, J.D., Hsu, B.B., Heeger, A.J., 2010. Proc. Natl. Acad. Sci. USA 107 (24), 10837–10841.
Xuan, F., Luo, X., Hsing, I.-M., 2012. Anal. Chem. 84 (12), 5216–5220.
Yin, P., Choi, H.M., Calvert, C.R., Pierce, N.A., 2008. Nature 451 (7176), 318–322.
Zhang, X., Liu, B., Dave, N., Servos, M.R., Liu, J., 2012. Langmuir 28 (49), 17053–17060.
Zhang, Y., Yan, Y.R., Chen, W.H., Cheng, W., Li, S.Q., Ding, X.J., Li, D.D., Wang, H., Ju, H. X., Ding, S.J., 2015. Biosens. Bioelectron. 68, 343–349.
Zhou, S., Wen, J., Chen, J., Lu, Q., 2015. Environ. Sci. Technol. Lett. 2 (2), 26–30.